J. Electrochem. Sci. Eng. **15(2)** (2025) 2620; http://dx.doi.org/10.5599/jese.2620

Open Access : : ISSN 1847-9286
https://pub.iapchem.org/ojs/index.php/JESE

Original scientific paper

MoS_2 nanosheets-modified screen-printed electrode for the simultaneous detection of carmoisine and tartrazine

Hussein Jassim Abboud[1], Zaid H. Mahmoud[2], Aya Mohammed Saadoun[3], Ekhlas A. Abdul Kareem[2], Mustafa Mudhafar[4,5], Qais R. Lahhob[6,✉] and Raed Muslim Mhaibes[7,✉]

[1]*Ministry of Education, Baghdad, Iraq*
[2]*University of Diyala, College of Sciences, Chemistry Department, Iraq*
[3]*Albayan University, Basic Science Departmwnt, Iraq*
[4]*Department of Medical Physics, Faculty of Medical Applied Sciences, University of Kerbala, 56001, Karbala, Iraq*
[5]*Department of Anesthesia Techniques and Intensive Care, Al-Taff University College, 56001, Kerbala, Iraq*
[6]*Collage of Pharmacy, National University of Science and Technology, Dhi Qar, 64001, Iraq*
[7]*Department of Biochemistry, College of Medicine, Misan University, Misan, Iraq*

Corresponding authors: ✉qaisrlahhob@gmail.com, ✉Raid.mcm@uomisan.edu.iq

Received: December 9, 2024; Accepted: January 4, 2025; Published: March 3, 2025

Abstract

Solvothermal synthesis was used to create molybdenum disulfide nanosheets (MoS_2 NSs). A screen-printed electrode (MoS_2 NSs / SPE) was modified using the produced MoS_2 nanosheets and employed as the working electrode for the voltammetric measurement of carmoisine. For the oxidation of carmoisine, the MoS_2 NSs/SPE showed increased electrocatalytic activity. With a detection limit as low as 0.03 µM under ideal circumstances, it was discovered that the oxidation peak currents of carmoisine were linearly proportional to its concentration in 0.1 to 400.0 µM. Additionally, the MoS_2 NSs / SPE showed promise for simultaneous detection of both chemicals by effectively identifying carmoisine even in the presence of tartrazine. The MoS_2 NSs / SPE was appropriate for simultaneous detection of tartrazine and carmoisine using differential pulse voltammetry as the oxidation peak potentials of the two azo dyes were adequately separated by 200 mV.

Keywords

Transition-metal dichalcogenide; Differential pulse voltammetry; electrochemical sensors, chemically modified electrodes, real sample analysis

Introduction

Food colorants, which are actually food additives, are extraneously added to food and drinks so as to improve their look through artificial coloration and produce the effect of the highest visual appealing to customers. For that reason, the food industry needed to apply various kinds of food-

grade colorants. These were mainly different in color and either natural or artificial [1]. Azodyes, a synthetic colouring agents, have been the prominent colorant used to improve the look and colour of food products, but due to their consistent color, low water solubility, low microbial contamination risk, low production costs, and excellent stability in the presence of light, oxygen, and pH changes, making them an ideal choice for food industries [1-5].

Coal tar pitch is the source of carmoisine, also known as E 122, a synthetic red azo dye that is widely used as a food and beverage colorant. It has functional groups, including hydroxy, sulpho, azo, and aromatic ring structures connected to possible negative health consequences when ingested in excess [6]. Carmoisine is used extensively as a food and beverage colorant since it is a highly water-soluble dye with exceptional stability that does not degrade even when exposed to light and oxygen. Carmoisine is classified as an emerging contaminant because of its stability and water solubility, which cause it to persist in aquatic habitats and raise questions about its possible effects on the environment and human health [7]. High levels of carmoisine exposure have been demonstrated to have detrimental impacts on health, such as carcinogenic effects that raise the chance of cancer, toxic effects that damage cells and tissues, and mutagenic effects that change genetic material [8].

E 102, another name for tartrazine, is an orange azo dye that dissolves in water and is frequently used as a colorant in a variety of goods, such as food, cosmetics, and medications. However, because of its widespread usage, it has been released into the environment through industrial effluent, which has contaminated water supplies. To reduce possible health hazards, the recommended daily intake of tartrazine in non-alcoholic drinks should not be more than 0.01 g/ml [9]. The possible hazards of consuming excessive amounts of tartrazine are highlighted by the fact that it has been connected to a number of human health issues, such as reproductive toxicity, alterations in kidney and liver function, and even neurobehavioral toxicity. The potential health risks associated with excessive consumption of tartrazine and carmoisine underscore the need for rigorous monitoring of their concentrations in relevant products. This requires the development and implementation of a rapid, simple, sensitive, and cost-effective analytical method to ensure the safety of consumers and prevent adverse health effects. Several analytical techniques are available for detecting and quantifying tartrazine and carmoisine, including spectrophotometry [10], HPLC [11] and capillary electrophoresis [12], each offering a unique set of advantages and capabilities for monitoring these synthetic colorants. Despite their effectiveness, many of these analytical techniques are often complex and labor-intensive, requiring specialized expertise and expensive equipment, making them less accessible and practical for routine monitoring and analysis.

Electrochemical sensing systems offer a range of advantages, including being cost-effective, portable, and simple to use, with benefits such as low limits of detection, fast analysis times, wide linear dynamic ranges, and high selectivity, even in the presence of interfering substances, making them an attractive option for analytical applications [13]. Voltammetric techniques, such as differential pulse voltammetry (DPV), offer several advantages, including rapid response times, high sensitivity, and excellent selectivity, making them a valuable tool for analytical determinations [14].

Screen-printing electrodes (SPEs) have been widely used for the large-scale production of disposable electrochemical sensors, offering a cost-effective and efficient way to manufacture sensing systems for various applications [15]. Screen-printing electrodes (SPEs) offer a unique combination of affordability, mass production capabilities, and sufficient reproducibility while also providing the benefits of versatility and miniaturization, making them an attractive option for the development of electrochemical sensing systems [15].

The bare electrode exhibits poor electrocatalytic performance [15]. Modifying the electrode surface significantly enhances its sensitivity, reproducibility, and overall stability [16]. The incorporation of nanomaterials can substantially boost the detection of trace analyte levels by dramatically improving the surface characteristics and electroconductivity of the electrodes [16].

Nanomaterials possess distinct physical and chemical properties, making them a popular choice for augmenting the sensing capabilities of electrochemical methods [17,18].

In recent years, there has been a surge of interest in two-dimensional (2D) nanomaterials, driven by their exceptionally thin and unique structure. Particular attention has been given to 2D MoS_2, a material composed of a single layer of molybdenum atoms sandwiched between two layers of hexagonally arranged sulphur atoms, forming a unique monoatomic structure. MoS_2, a two-dimensional layered transition-metal dichalcogenide, exhibits outstanding electrical properties and remarkable optical characteristics, making it a highly promising material [19]. The top gate configuration of layered MoS_2 crystals often yields exceptionally high electronic performance, characterized by impressive on-off ratios comparable to those of graphene nanoribbons. Furthermore, due to their high surface-to-volume ratios, these graphene-like materials may offer the potential for ultra-high sensitivity in detecting a wide range of biological, dietary, and environmental compounds [20].

In order to detect carmoisine, this study suggested using MoS_2 nanosheets (NSs) in conjunction with a screen-printed electrode (SPE). It is crucial to note that DPV, chronoamperometry, and CV were among the electrochemical methods used to assess the electrochemical characteristics of carmoisine and the performance of the MoS_2 NSs/SPE. Subsequent research showed that the MoS_2 NSs/SPE sensor had both exceptional electrocatalytic activity for carmoisine and the capacity to detect carmoisine and tartrazine in combination with different and recognizable signals. The MoS_2 NSs/SPE sensor's promise for practical uses was demonstrated when it was successfully used to accurately determine the levels of tartrazine and carmoisine in real samples.

Experimental

Apparatus and chemicals

An Autolab potentiostat/galvanostat was used for electrochemical experiments. A three-electrode setup including a graphite working electrode (WE), a graphite auxiliary electrode (AE), and a silver pseudo-reference electrode (RE) was used in the screen-printed electrodes (SPEs) manufactured by DropSens (DRP-110, Spain). A Metrohm 710 pH meter was used to measure the pH. Every solution was made from scratch with double-distilled water. All chemicals used, including tartrazine and carmosine, were analytical grade and came from Merck. Orthophosphoric acid and its salts purchased from Merck were used to make the buffer solutions.

Synthesis of MoS_2 NSs

To synthesize MoS_2 NSs, 0.26 g of ammonium molybdate and 0.50 g of thiourea were first dissolved in 30 ml of deionized - water through 15 min of stirring. The resulting solution was then transferred to an autoclave, which underwent hydrothermal treatment at 190 °C for about 24 h. After the hydrothermal reaction, the sediments were collected, repeatedly washed with ethanol, and dried under vacuum at 65 °C overnight.

Preparation of MoS_2 NSs / SPE

To achieve this, 2 mg of MoS_2 NSs were dispersed in 1 milliliter of ultra-pure water through 15 min of dispersion. Subsequently, the working electrode was fabricated by casting 5 microliters of the MoS_2

NSs suspension onto it. The modified electrode was then obtained by allowing the solvent to evaporate. The MoS_2 NSs / SPE was formed after the evaporation of the solvent.

Preparation of real samples

15.0 ml of lemon juice was filtered using filter paper to create a sample. Next, 2.0 ml of PBS was mixed with 10.0 ml of the filtered sample to dilute it.

Six grams of the powder were dissolved in 70 ml of deionized water at fifty degrees Celsius in order to create a powdered juice sample. 10 ml of PBS was then added to the solution to further dilute it. A 0.45-micrometer membrane filter was then used to filter the diluted solution.

Results and discussion

The MoS_2 NSs were subjected to X-ray diffraction (XRD) examination in order to investigate the crystal structure of the produced material. As illustrated in Figure 1, the prepared sample's XRD pattern shows prominent diffraction peaks at 2θ values of 14.0, 33.5, 39.8, 42.9, 49.3, 59.1 and 69.6°. These values correspond to the hexagonal MoS_2 structure's (002), (100), (103), (006), (105), (110), and (200) planes and match the standard pattern (JCPDS 37-1492) [21].

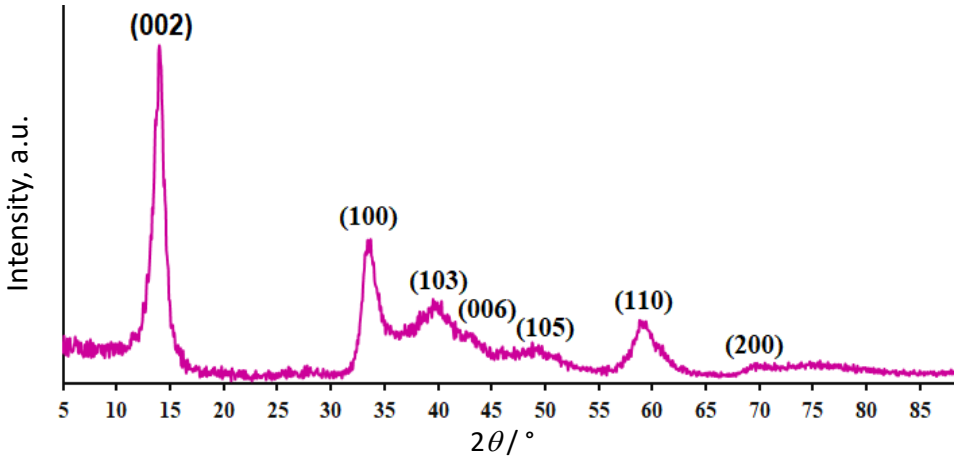

Figure 1. *X-ray diffraction (XRD) pattern of MoS_2 nanosheets (NSs)*

The produced MoS_2 NSs sample's FE-SEM pictures at various magnifications are shown in Figure 2.

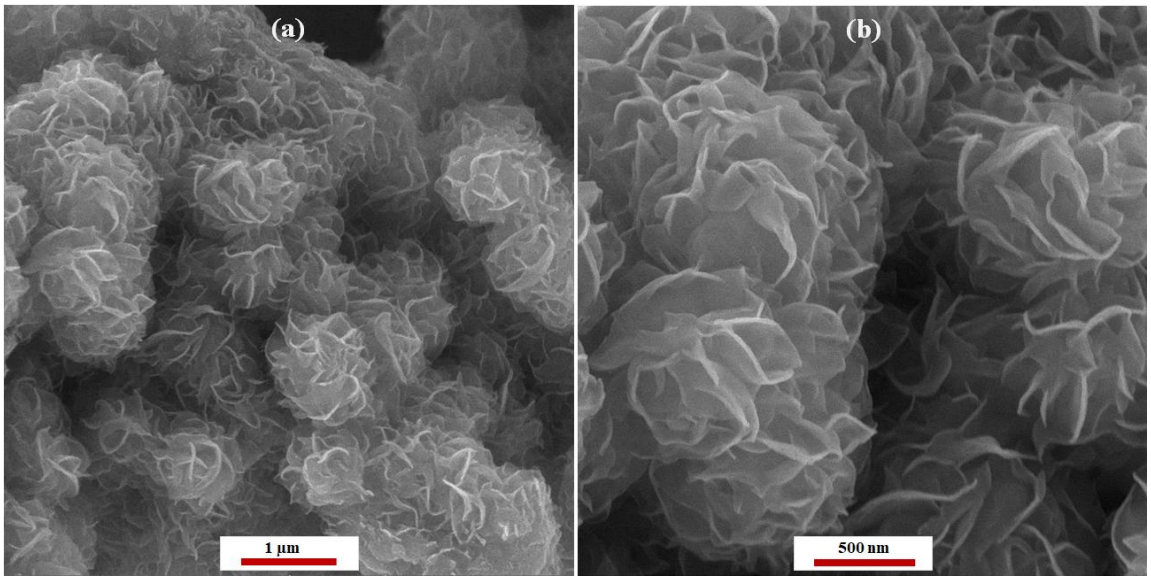

Figure 2. *Field emission scanning electron microscopy images of MoS_2 nanosheets at different magnifications a) 1 µm and b) 500 nm*

The generated MoS_2 sample has spherical-like structures made up of many integrated nano-sheets, as seen by the FE-SEM pictures.

Cyclic voltammetric study of carmoisine oxidation

Figure 3 shows the CVs for the electrochemical oxidation of 100.0 µM carmoisine at the bare screen-printed electrode (SPE) (curve a) and the MoS_2 NSs-modified SPE (curve b). A comparison of the two curves reveals that the anodic peak potential for carmoisine oxidation at the MoS_2 NSs-modified SPE (curve b) is approximately 480 mV, which is significantly lower than the peak potential observed at the bare SPE (curve a), which is around 630 mV. A similar trend is observed for carmoisine oxidation, where the anodic peak current at the MoS_2 NSs-modified SPE (curve b) is substantially higher than the bare SPE (curve a), indicating a significant enhancement in the electrochemical response at the modified electrode. The results clearly demonstrate that the modification of the SPE with MoS_2 NSs significantly enhances the electrochemical characteristics of carmoisine oxidation, indicating improved performance of the modified electrode.

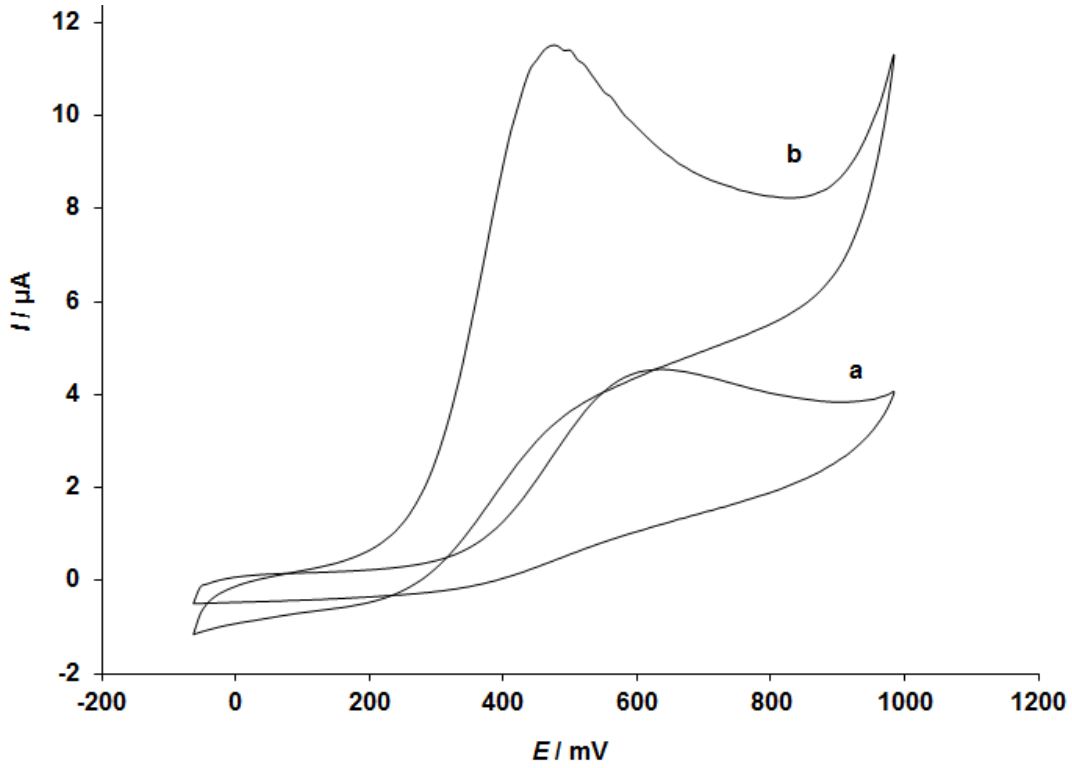

Figure 3. *CVs of 100.0 µM carmoisine at the surface of the unmodified screen-printed electrode (SPE) (a) and the MoS_2 NSs-modified SPE (b)*

Effect of scan rate

The investigation was done with linear sweep voltammetry (LSV) and the effect of potential sweep rate on oxidation of carmoisine at the MoS_2 NSs-modified SPE is mentioned; the findings are shown in Figure 4A. It can be seen from a plot of the peak current (I_p) against the $v^{1/2}$ (5 to 400 mV/s) that oxidation of carmoisine at the MoS_2 NSs-modified SPE is not a diffusion-controlled process anymore but rather is a surface-controlled one at the overpotential, which is a sufficient value (Figure 4B).

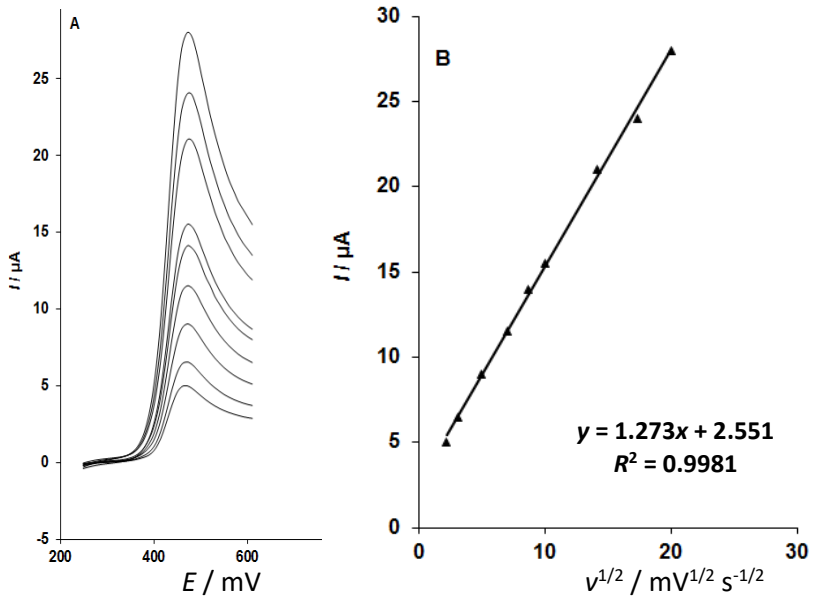

Figure 4. *(A) shows the MoS_2 NSs-modified SPE's linear sweep voltammograms (LSVs) at scan rates of 5.0, 10.0, 25.0, 50.0, 75.0, 100.0, 200.0, 300.0, and 400.0 mV/s in 100.0 µM carmoisine. (B) I against $v^{1/2}$*

Chronoamperometric measurements

Chromatoamperometric experiments were conducted for carmoisine at the MoS_2 NSs-modified SPE. The current responses resulting from different carmoisine concentrations were recorded (Figure 5A).

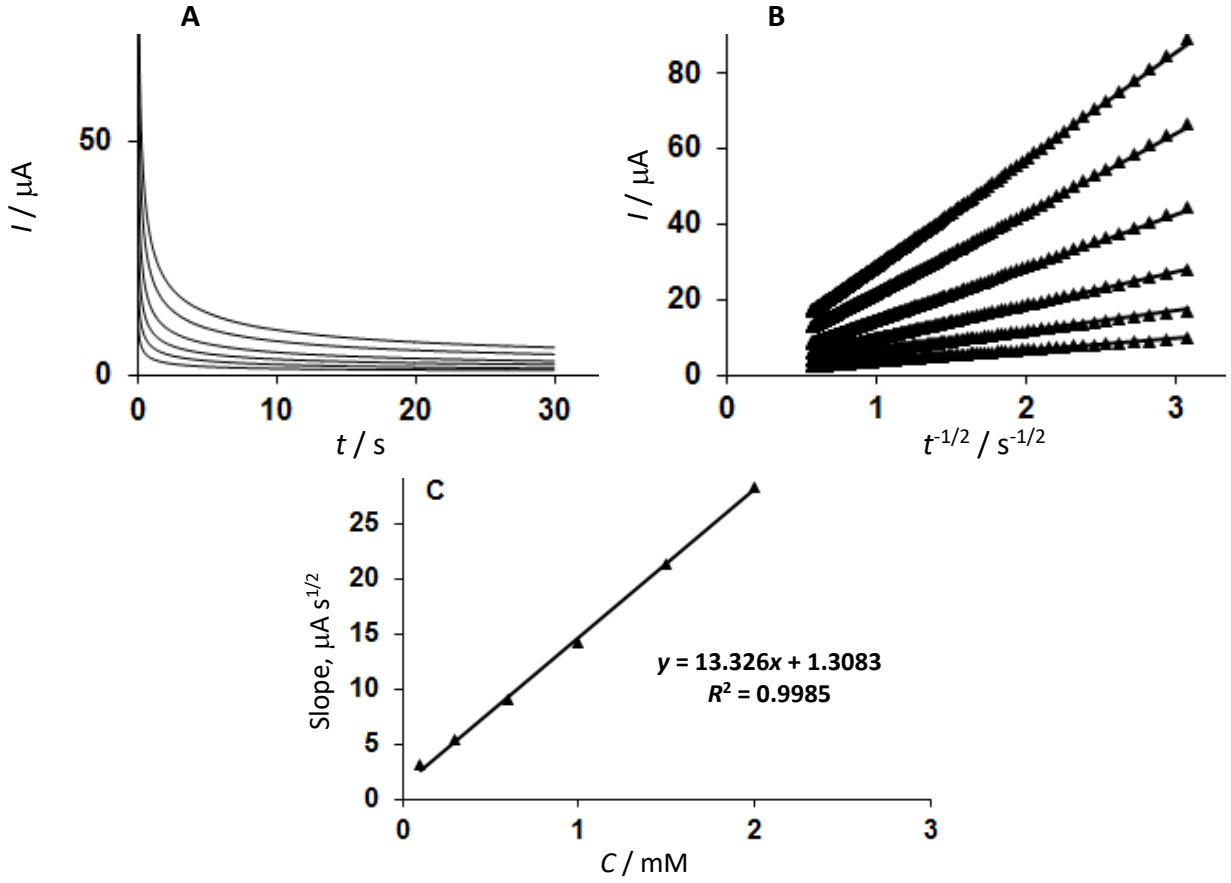

Figure 5. *(A) Chronoamperometric responses obtained at the MoS_2 NSs-modified SPE for various concentrations of carmoisine (0.1, 0.3, 0.6, 1.0, 1.5, and 2.0 mM). (B) Cottrell plots of current versus $t^{-1/2}$ derived from the chronoamperograms. (C) Calibration plot of the slope of the straight lines from the Cottrell plots against carmoisine concentration*

For carmoisine, the current-time response under mass transport limited conditions can be described by Cottrell Equation (1) [22]:

$$I = nFAD^{1/2}C/\pi^{-1/2}t^{-1/2} \quad (1)$$

The best fits for various carmoisine concentrations are displayed in Figure 5B, which is an experimental plot of current (I) against the inverse square root of time ($t^{-1/2}$). A curve was created by plotting the slope that emerged from the Cottrell plots (Figure 5B) against the carmoisine concentration (Figure 5C). The mean diffusion coefficient (D) of carmoisine was determined to be 6.1×10^{-5} cm²/s using the Cottrell equation and the slope derived from the calibration curve (Figure 5C).

Calibration plot and LOD

The quantitative measurement of carmoisine in solution can be based on the electrocatalytic peak current for carmoisine oxidation at the MoS_2 NSs-modified SPE. In order to do this, investigations utilizing the MoS_2 NSs-modified SPE with varying carmoisine concentrations were carried out using differential pulse voltammetry (DPV) (Figure 6A). A linear association with a slope of 0.1021 µA/µM was found for the concentration range of 0.1 to 400.0 mM. It was determined that the detection limit (3σ) was 0.03 µM (Figure 6B). The findings of some recent work on the electrochemical determination of carmoisine are displayed in Table 1.

Table 1. *Comparison the values of LOD and linear range of the MoS_2 NSs-modified SPE sensor with some of the previously published reports*

Modified electrode	Linear range, µM	LOD, µM	Ref.
$CaMgFe_2O_4$ hollow spheres-modified carbon paste electrode	10 to 900	0.86	[23]
Mesoporous Pr_6O_{11}/Ionic liquid/carbon paste electrode	0.09 to 135.00	0.0012	[24]
MoS_2 NSs-modified SPE	0.1 to 400.0	0.03	This work

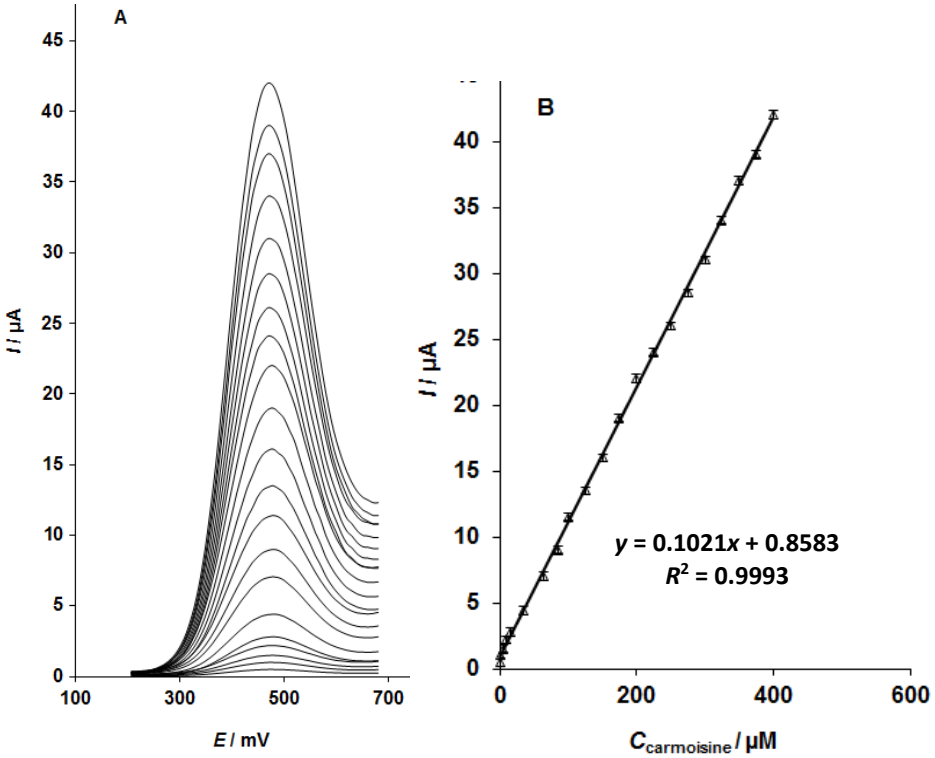

Figure 6. *(A) Differential pulse voltammograms (DPVs) of the MoS_2 NSs-modified SPE containing various concentrations of carmoisine (0.1, 1.0, 5.0, 10.0, 15.0, 35.0, 65.0, 85.0, 100.0, 125.0, 150.0, 175.0, 200.0, 225.0, 250.0, 275.0, 300.0, 325.0, 350.0, 375.0, and 400.0 µM). (B) Calibration plot of peak current versus carmoisine concentration*

Simultaneous determination of carmoisine and tartrazine

No prior research has used MoS_2 NSs-modified SPE for the simultaneous analysis of carmoisine and tartrazine, and this is the first report on its application. As seen in Figure 7A, the simultaneous measurement of carmoisine and tartrazine was accomplished by altering the concentrations of both substances concurrently and recording the resulting differential pulse voltammograms (DPVs). The oxidation of carmoisine and tartrazine was represented by distinct anodic peaks in the voltammetric findings, which were obtained at potentials of 480 mV and 1170 mV. As shown in Figure 7A, this suggests that the MoS_2 NSs-modified SPE can identify these two chemicals at the same time.

The MoS_2 NSs-modified SPE's sensitivity to carmoisine oxidation was found to be 0.1031 µA/µM, quite near the value measured without tartrazine. This implies that these chemicals' oxidation processes at the MoS_2 NSs/SPE are separate, making it possible to determine their mixes simultaneously without experiencing any major interferences.

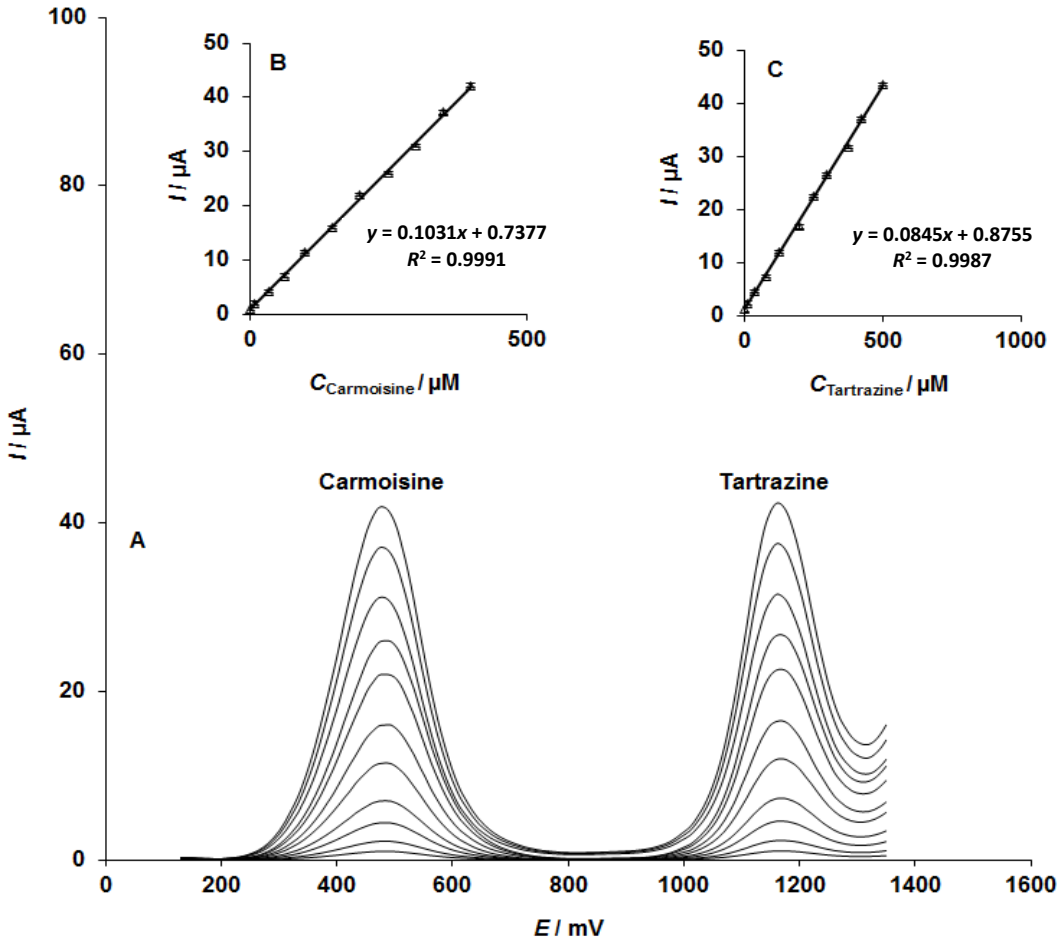

Figure 7. *(A) DPVs of the MoS_2 NSs-modified, containing different concentrations of carmoisine and tartrazine (in µM), from inner to outer: 1.0+2.0, 10.0+15.0, 35.0+40.0, 65.0+80.0, 100.0+125.0, 150.0+200.0, 200.0+250.0, 250.0+300.0, 300.0+375.0, 350.0+425.0, and 400.0+500.0, respectively. Insets: (B) Plot of Ip versus carmoisine concentration and (C) Plot of Ip versus tartrazine concentration*

Stability, reproducibility, and repeatability

The MoS_2-NSs-modified SPE was air-stored at ambient conditions in order to verify its stability using the DPV technique. According to the findings, the modified electrode's peak carmoisine current (40.0 µM) retained 97.5 % of its initial current after a week, indicating the sensor's remarkable long-term stability. Ten separate voltammetric measurements were made to assess the carmoisine electro-oxidation (40.0 µM) on the same MoS_2 NSs-modified SPE electrode. The findings

showed that the generated sensor was highly repeatable, with an RSD of 3.4 %. The carmoisine response currents (40.0 µM) on five MoS_2-modified SPE were compared under the same circumstances, and the findings demonstrated the remarkable repeatability of the generated sensor with an RSD of 3.7 %.

Interference study

It was examined how different alien species affected the measurement of 50.0 µM carmoisine. With a relative inaccuracy of about ±5 %, the tolerance limit was calculated as the highest concentration of invasive species. According to the results, there was no interference and the sensor's strong selectivity for carmoisine analysis was confirmed for Li^+, Na^+, Ca^{2+}, F^-, Br^-, Fe^2, Mg^{2+}, Zn^{2+}, K^+, Cl^-, NO_3^-, SO_4^{2-}, Mn^{2+}, Ca^{2+}, citric acid, glucose, tryptophan, pantothenic acid, thiamine, indigo carmine and brilliant blue.

Determination of carmoisine and tartrazine in real samples

The mentioned procedure was implemented in the analysis of carmoisine and tartrazine in real samples, viz. powdered juice and lemon juice, to attempt its real analytic power. Table 2 contains the results of the analysis of tartrazine and carmoisine in the lemon juice and powdered juice samples. The accuracy and dependability of the suggested approach were evident from the satisfactory recovery rates achieved during the measurement of carmoisine and tartrazine in actual peptides. The repeatability of the approach was assessed by measuring the RSD, which was another way of making sure that the measurement was accurate, showing at the same time the reliability and dependability of the suggested approach.

Table 2. *Results of the estimation of carmoisine and tartrazine in powdered juice and lemon juice samples using the MoS_2 NSs / SPE method. The results are based on five replicate measurements (*n=*5).*

	Concentration, µM				Recovery, %		RSD, %	
	Spiked		Found					
Sample	Carmoisine	Tartrazine	Carmoisine	Tartrazine	Carmoisine	Tartrazine	Carmoisine	Tartrazine
Powdered juice	0	0	3.1	3.9	-	-	3.3	2.7
	2.0	1.0	5.0	5.1	98.0	104.1	2.7	3.1
	4.0	3.0	7.3	6.7	102.8	97.1	1.9	2.9
	6.0	5.0	8.9	9.1	97.8	102.3	3.0	2.4
	8.0	7.0	11.2	10.7	100.9	98.2	2.4	2.5
Lemon juice	0	0	-	4.1	-	-	-	3.4
	5.0	2.0	5.1	6.0	102.0	98.4	2.0	1.8
	7.5	3.0	7.3	7.3	97.3	102.8	2.2	2.9
	9.5	4.0	9.4	8.0	98.9	98.7	3.3	2.7
	11.5	5.0	11.6	8.8	100.9	96.7	1.9	3.5

Conclusions

This work presents a simple process for creating molybdenum disulfide nanosheets (*MoS_2* NSs), which were subsequently used with a screen printed electrode (SPE) to detect carmoisine electrochemically using voltammetry. MoS_2 NSs and SPE work together to provide a very efficient carmoisine detection system, and their synergy improves the system's overall detection capabilities. A broad and efficient detection range was shown by the developed sensor's linear response to carmoisine concentrations ranging from 0.1 to 400.0 µM.

References

[1] M. V. Vieira, S. Noore, B. Tiwari, C. O'. Donnell, C. Gonçalves, L. M. Pastrana, P. Fuciños, Enhancing the stability and functionality of phycobili proteins as natural food colourants

through microparticle formulation, *Food Chemistry* **465** (2025) 142077. https://doi.org/10.1016/j.foodchem.2024.142077

[2] P. Barciela, A. Perez-Vazquez, M. A. Prieto, Azo dyes in the food industry: Features, classification, toxicity, alternatives, and regulation, *Food and Chemical Toxicology* **178** (2023) 113935. https://doi.org/10.1016/j.fct.2023.113935

[3] R. B. Shakuntala, J. Keshavayya, K. M. Mussuvir Pasha, N. D. Satyanarayan, B. N. Nippu, B. Thippeswamy, Synthesis, Spectroscopic, Computational, and Biological Evaluation of Pyrazole mono azo dyes, *Journal of Molecular Structure* **1309** (2024) 138045. https://doi.org/10.1016/j.molstruc.2024.138045

[4] S. D. Nagesh, D. Satheesh, R. Devi Ravi, R. Pachaiappan, K. Manavalan, L. Cornejo-Ponce, T. Sethuramachandran, An effective photocatalytic decomposition of azo dyes by NiO/ZnO/g-C_3N_4 ternary nanocomposite under solar light excitation, *Surfaces and Interfaces* **56** (2024) 105578. https://doi.org/10.1016/j.surfin.2024.105578

[5] P. Vineis, R. Pirastu, Aromatic amines and cancer, *Cancer Causes Control* **8** (1997) 346-355. https://doi.org/10.1023/A:1018453104303

[6] S. Sunil, B. Kumar Mandal, Facile synthesis of CQD/g-C_3N_4 as a highly effective metal-free photocatalyst for the degradation of carmoisine and indigo carmine dye, *Inorganic Chemistry Communications* **171** (2025) 113545. https://doi.org/10.1016/j.inoche.2024.113545

[7] H. Barrera, J. Cruz-Olivares, B. A. Frontana-Uribe, A. Gomez-Diaz, P. G. Reyes-Romero, C. E. Barrera-Diaz, Electrooxidation-plasma treatment for azo dye carmoisine (Acid Red 14) in an aqueous solution, *Materials* **13** (2020) 1463. https://doi.org/10.3390/ma13061463

[8] G. P. Ford, B. I. Stevenson, J. G. Evans, Long-term toxicity study of carmoisine in rats using animals exposed in utero, *Food and Chemical Toxicology* **25** (1987) 919-925. https://doi.org/10.1016/0278-6915(87)90285-7

[9] K. Rovina, S. Siddiquee, S. M. Shaarani, A review of extraction and analytical methods for the determination of tartrazine (E 102) in foodstuffs, *Critical Reviews in Analytical Chemistry* **47** (2017) 309-324. https://doi.org/10.1080/10408347.2017.1287558

[10] Z. Kiayi, T. Bagheri Lotfabad, A. Heidarinasab, F. Shahcheraghi, Microbial degradation of azo dye carmoisine in aqueous medium using Saccharomyces cerevisiae ATCC 9763, *Journal of Hazardous Materials* **373** (2019) 608-619. https://doi.org/10.1016/j.jhazmat.2019.03.111

[11] F. Turak, M. Dinç, O. Dülger, M. O. Özgür, Four derivative spectrophotometric methods for the simultaneous determination of carmoisine and ponceau 4R in drinks and comparison with high performance liquid chromatography, *International Journal of Analytical Chemistry* **2014** (2014) 650465. https://doi.org/10.1155/2014/650465

[12] H. Y. Huang, Y. C. Shih, Y. C. Chen, Determining eight colorants in milk beverages by capillary electrophoresis, *Journal of Chromatography A* ***959*** (2002) 317-325. https://doi.org/10.1016/S0021-9673(02)00441-7

[13] F. Yang, S. Li, X. Zhang, L. Wang, S. Liu, Single-particle collision electrochemical biosensing for DNA and protein kinase via sulfhydryl group manipulation and biomodification-free Pt nanoparticle, *Sensors and Actuators B* **426** (2025) 137099. https://doi.org/10.1016/j.snb.2024.137099

[14] C. Yengin, F. Gulay Der, I. Alcin, B. Cihan, E. Kilinc, Non-invasive electrochemical immunosensor for reverse iontophoretic determination of cardiac troponins (cTnT & cTnI) in a simulated artificial skin model, *Talanta* **256** (2023) 124276. https://doi.org/10.1016/j.talanta.2023.124276

[15] P. Kelíšková, O. Matvieiev, L. Janíková, R. Šelešovská, Recent advances in the use of screen-printed electrodes in drug analysis: A review, *Current Opinion in Electrochemistry* **42** (2023) 101408. https://doi.org/10.1016/j.coelec.2023.101408

[16] J. P. Chandhana, M. Roshith, S. P. Vasu, D. V. Ravi Kumar, T. G. Satheesh Babu, High aspect ratio copper nanowires modified screen-printed carbon electrode for interference-free non-enzymatic detection of serum creatinine in neutral medium, *Journal of Electroanalytical Chemistry* **971** (2024) 118605. https://doi.org/10.1016/j.jelechem.2024.118605
[17] X. Shi, Lei Shi, J. Wang, Y. Zhou, S. Zhao, Defect engineering of nanomaterials for selective electrocatalytic CO_2 reduction, *Matter* **7** (2024) 4233-4259. https://www.cell.com/matter/fulltext/S2590-2385(24)00492-2
[18] Y. Song, C. Tang, T. Wang, Y. Liu, X. He, C. Xie, G. Chen, C. Deng, Z. He, J. Huang, Nano FeNi-OH/$Co(OH)_2$/NF p-n heterojunction for efficient oxygen evolution reaction and electrocatalytic urea oxidation: Built-In electric field regulated charge distribution and mechanism exploration, *Applied Surface Science* **670** (2024) 160649. https://doi.org/10.1016/j.apsusc.2024.160649
[19] A. T. Ezhil Vilian, B. Dinesh, S. M. Kang, U. Maheswari Krishnan, Y. S. Huh, Y. K. Han, Recent advances in molybdenum disulfide-based electrode materials for electroanalytical applications, *Microchimica Acta* **186** (2019) 203. https://doi.org/10.1007/s00604-019-3287-y
[20] Z. Xie, S. Yu, X. Ma, K. Li, L. Ding, W. Wang, D.A. Cullen, H.M. Meyer III, H. Yu, J. Tong, Z. Wu, F.Y. Zhang, MoS_2 nanosheet integrated electrodes with engineered 1T-2H phases and defects for efficient hydrogen production in practical PEM electrolysis, *Applied Catalysis B: Environmental* **313** (2022) 121458. https://doi.org/10.1016/j.apcatb.2022.121458
[21] M. Dinesh, K. Muthumalai, Y. Haldorai, R. Thangavelu Rajendra Kumar, MoS2 nanosheets decorated multi-walled carbon nanotube composite electrocatalyst for 4-nitrophenol detection and hydrogen evolution reaction, *Electroanalysis* **32** (2020) 2571-2580. https://doi.org/10.1002/elan.202060351
[22] A .J. Bard, L. R. Faulkner, *Electrochemical Methods Fundamentals and Applications*, John Wiley & Sons, Inc., New York, USA, 2000. ISBN 978-0-471-04372-0
[23] M. Karami, M. Shabani-Nooshabadi, Electro-sensing of carmoisine and tartrazine in foodstuffs based on triple-shell $CaMgFe_2O_4$ hollow spheres-modified sensor, *Materials Chemistry and Physics* **318** (2024) 129289. https://doi.org/10.1016/j.matchemphys.2024.129289
[24] S. Hamzeh, H. Mahmoudi-Moghaddam, S. Zinatloo-Ajabshir, M. Amiri, S. A. Razavi Nasab, Eco-friendly synthesis of mesoporous praseodymium oxide nanoparticles for highly efficient electrochemical sensing of carmoisine in food samples, *Food Chemistry* **433** (2024) 137363. https://doi.org/10.1016/j.foodchem.2023.137363